(a) $$F_2' = \frac{\int F_2 G_2 df}{\int G_2 df},$$

which would reduce to $F_2' = F_2$, if F_2 were constant at all frequencies. Actually, it is not, but the ratio F_2'/F_2 approaches unity as the bandwidth is decreased.

Arbitrarily, a bandwidth of 0.25 mc was chosen at an IF frequency of 30 mc, which is less than 1 per cent bandwidth. Under these conditions calculated values of the ratio are:

$$\frac{F_{2s}'}{F_{2s}} = 1.00093, \text{ for } p = 1$$

$$\frac{F_2'}{F_2} = 1.00081, \text{ for } p = 2.$$

The error in assuming $F_2'/F_{2s}' = F_2/F_{2s}$ is much less than either of the above errors, since the error in F_2' and that in F_{2s}' are in the same direction.

(b) For same bandwidth of 0.25 mc calculations show

$$\frac{\eta \int U df}{\int \eta U df} = 1.0040, \text{ for } p = 1 \text{ and}$$

$$= 1.0025, \text{ for } p = 2.$$

In actual calculations of total noise power, $KT_0\eta\int Udf$ is added to a constant term arising from the shot effect; consequently the error in the total output noise power will be less than indicated by the values of the ratio shown above. Further, since the Y factor is the ratio of two such expressions, with their respective errors lying in the same direction, the error in the Y factor itself will be much less. From these considerations it would appear that the error in Y factor resulting from the second assumption is not greater than about 0.1 per cent.

Appendix III

List of Symbols Not Explicitly Defined in the Text

G_1 = conversion gain of the crystal.
G_2 = available-power gain of the IF amplifier and output meter when driven by a signal generator whose internal conductance is equal to that of the crystal.
G_{2s} = available-power gain of the IF amplifier and output meter when driven by a generator of internal conductance g_s.
F_2' = effective noise figure of the IF amplifier with a resistor on the input.
F_{2s}' = effective noise figure of the IF amplifier with a standard resistor on the input.
(*Note*—unprimed F symbols refer to the noise figure for an incremental frequency band df.)
N_0 = output noise power of the over-all network with a crystal on the input.
N_{0s} = output noise power of the over-all network with a standard resistor on the input.
N_{0N} = output noise power of the over-all network with a crystal on the input driven by a diode noise source.
g_1' = IF conductance of a crystal.
g_s = standard IF conductance.
g_1 = conductance at output of the Roberts line with a conductance g_1' on the input.
g_a = conductance at the output of the Roberts line with a standard conductance g_s on the input.
b = susceptance at the output of the Roberts line with a conductance g_1' on the input ($b = 0$ for $g_1' = g_s$).

Circuit Components in Dielectric Image Lines

D. D. KING†

Summary—Symmetry of dipole mode in a dielectric rod permits use of an image system. By replacing lower half of dielectric and its surrounding field with an image surface, support problem is eliminated. Resulting image provides structural convenience and also has very low loss, provided wave is allowed to occupy a cross section many wavelengths square. In millimeter region this is readily achieved. Possibilities of new types of circuit elements in this image system are explored. Combination of optical and waveguide techniques is a characteristic of resulting components. Properties of several transducers between image line and either rectangular waveguide or coaxial line are described. Attenuators, standing-wave detector, and various directional coupler types for image lines are also discussed.

† Radiation Lab., Johns Hopkins University, Baltimore 18, Md.

Introduction

THE HE_{11} or dipole mode in a thin dielectric rod offers very low attenuation and freedom from higher modes. This mode possesses a plane of symmetry, and hence may be operated as an image system.[1] The cross section of an image line is shown in Fig. 1. Only the E field in the dielectric is indicated. The complete mode pattern is complicated, since all three components of E and H are present. The theory of the dipole mode

[1] D. D. King, "Dielectric Image Line" (letter), *Jour. Appl. Phys.*, vol. 23, p. 699; June, 1952.

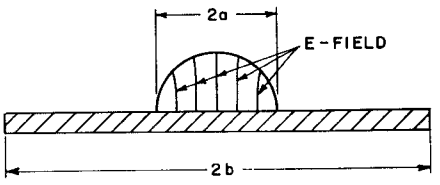

Fig. 1

has been worked out by Elsasser,[2] and shows continuously decreasing attenuation as the dielectric cross section is reduced. This is a consequence of the extension of the field into the space around the dielectric where no losses occur. In the limit of vanishing dielectric and zero attenuation we have an infinite plane wave which is of no practical use. However, at short wavelengths, very low loss can be achieved within an acceptable cross section. An attenuation curve is shown in Fig. 2, together with a point measured on an image system.

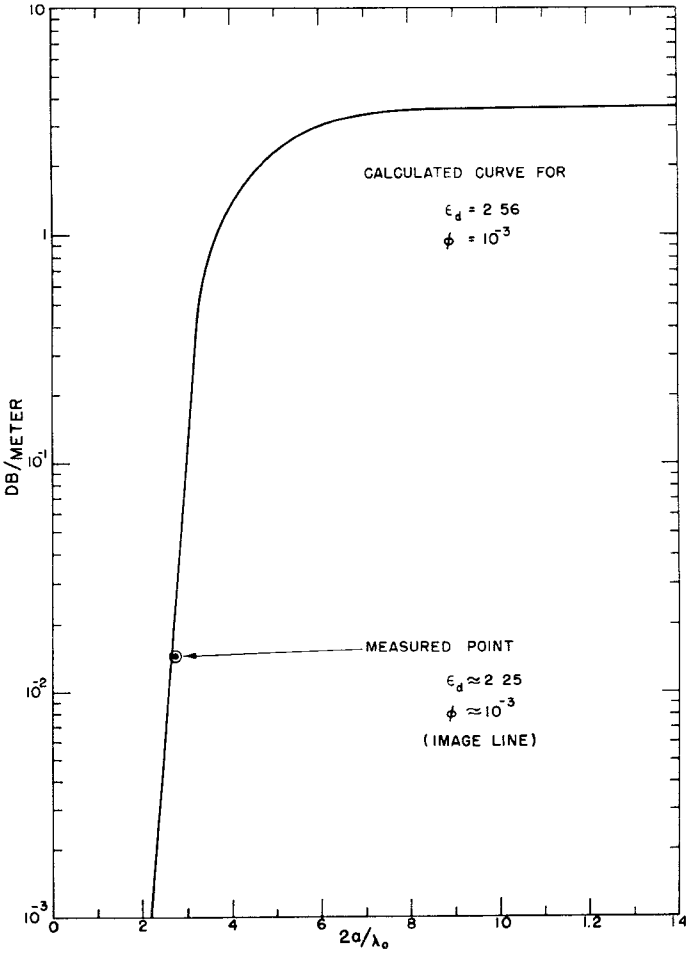

Fig. 2

The properties of dielectric image line in straight sections, bends and twists have been briefly described previously.[3] The results obtained show that the image system is very easy to construct, and permits compact bends of moderate loss and low reflections. Since the wave extends over a large cross section outside the dielectric, the system is insensitive to minor twists and imperfection in the dielectric itself. In this paper we shall describe circuit components for the image line and give preliminary data on their performance. These components include a transition directly to a coaxial crystal mount, attenuators, a standing-wave detector, and a directional coupler. These devices show clearly the joining of optical and waveguide methods which characterizes the image line. The ease with which the optical limit may be approached with this type of waveguide is particularly valuable in the millimeter region. Indeed, dielectric image line and its associated components in many ways bridge the gap between optical and waveguide techniques.

Transitions from Image Line to Rectangular Guide and Coaxial Line

The transition from waveguide to image line is best accomplished through a horn, as shown in Fig. 3. The added section for inserting the dielectric strip is only for convenience in moving the dielectric relative to the horn. The dielectric may equally well be permanently fastened to the waveguide wall. However, it must extend into the guide for several wavelengths to provide proper excitation of the dipole mode.

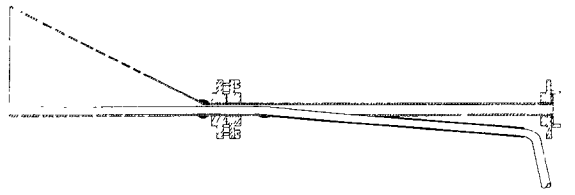

Fig. 3

The field on the image line is loosely coupled to the rod, and approximates a plane wave. Therefore, in addition to a horn, it is logical to consider a parabolic reflector as a launcher or receiver. The presence of the image surface permits easy access to the focus without obstructing the aperture. A pin transition from image line to waveguide is shown in Fig. 4. Probably because

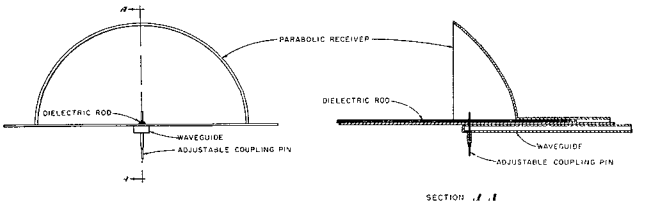

Fig. 4

of the thin pin, this transition proved lossy and sensitive to tuning. The best that could be achieved was an input voltage standing-wave ratio (VSWR) of about 1.3 and a loss of 5 db greater than the horn. A standard single-tuned crystal mount (PRD 621) was used in each.

The excitation of a rectangular guide by a pin followed by a similar transition to the center conductor of

[2] W. M. Elsasser, "Attenuation in a dielectric circular rod," *Jour. Appl. Phys.*, vol. 20, p. 1192; December, 1949.
[3] D. D. King, "Properties of dielectric images lines," Trans. IRE, vol. MTT 3, no. 2; March, 1955.

the coaxial crystal seems redundant. Therefore, in a modified transition the coupling pin is extended to contact the crystal directly. This eliminates the intervening waveguide. The resulting transducer appears in Fig. 5.

The dc return for the crystal was first extended upward through the reflector by means of a thin steel wire. This structure may be tuned by a slug placed on the thin wire. When properly adjusted, this mount proved to be only 3 db less efficient than the horn with tuned waveguide mount (PRD type 621).

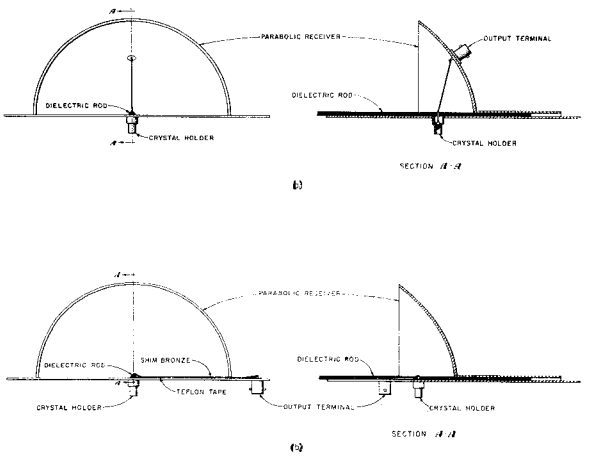

Fig. 5

In order to take full advantage of the image plane, a dc return path along the image surface can be provided. This circuit is also shown in Fig. 5. Here a thin strip of copper is placed on the image surface. A teflon tape insulates the ground plane and provides the bypass capacitance. A more refined design with recessed mounting of the strip is hardly necessary. The arrangement shown provides an input VSWR of 1.2 and a sensitivity superior to that of the horn with tuned waveguide mount.

Only the crystal position is used to tune the system. Of course, the location of parabolic reflector also determines the output, which is maximized when the probe is at the focus. However, a number of subsidiary maxima occur when the focus is located behind the probe. This indicates large standing waves on the dielectric between the probe and the base of the reflector.

Attenuators

A satisfactory attenuator or pad can be produced by placing a resistance card on the image surface, as shown in Fig. 6. Placing the resistance coating uppermost increases the effect. However, a plain bakelite sheet serves quite well without any resistance coating.

A calibrated attenuator appears possible from an inspection of the field components. Thus, we find that in the cross section, the electric field components have the following dependence on the polar angle:

$$E_z \sim \cos\psi$$
$$E_\rho \sim \cos\psi$$
$$E_\psi \sim \sin\psi.$$

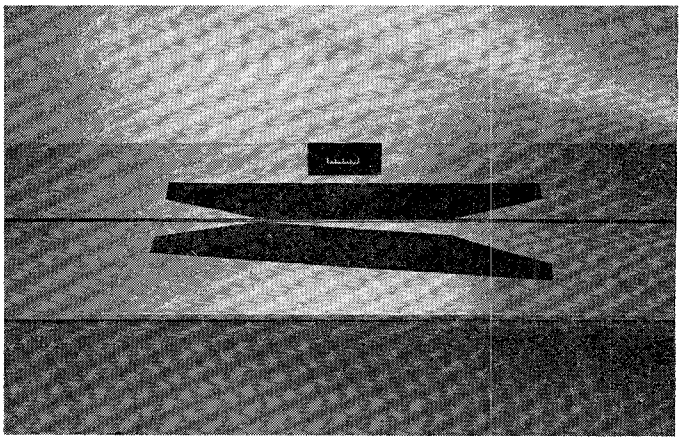

Fig. 6

If a thin resistive sheet is placed in a radial plane, then only tangential components of E field, *i.e.*, E_ρ and E_z, should be attenuated. Attenuation introduced by resistance element will then be proportional to $\cos^2\psi$.

An attenuator of this type is shown in Fig. 7. The performance achieved depends greatly on the size and resistance of the sheet used. Generally, the cosine dependence is not observed. A typical response curve is shown in Fig. 8. The behavior is probably due to a rotational disturbance of the original mode by the card. A distortion of the field will, of course, destroy the pure cosine dependence required for proper operation of this type of attenuator.

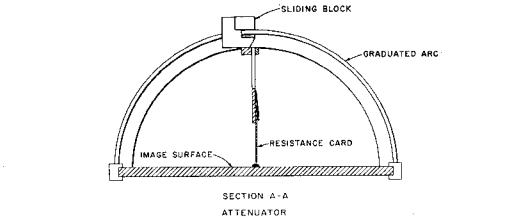

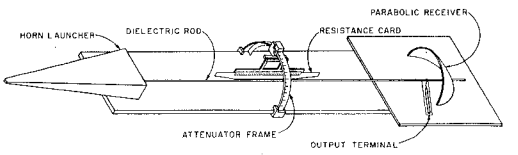

Fig. 7

ATTENUATOR CHARACTERISTICS

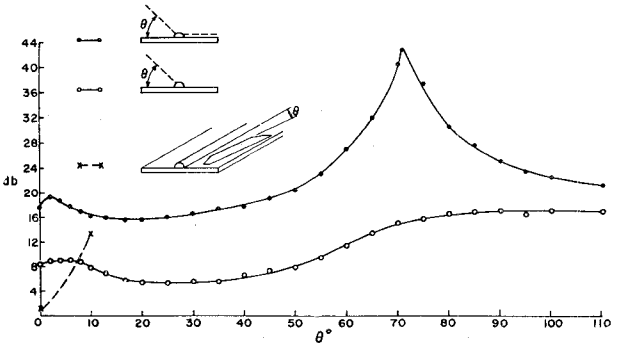

Fig. 8

Standing-Wave Detector

A direct measurement of the standing waves along the line is possible in several ways. A radial probe in the plane perpendicular to the image surface was first tried. The mounting of this probe on a carriage is awkward, and a long probe is required to reach the dielectric from above. The probe must reach near the dielectric surface to follow the sharp minimum in large values of vswr. Presumably, stray coupling obscures the minimum unless the end of the probe extends to the dielectric. This type of external probe does not take advantage of the image symmetry, and was replaced by the slotted system described below.

To determine the effect of an axial slot in the image surface, we must examine the H-field components. The dependence of these is given below:

$$H_z \sim J_1(k\rho) \sin \psi$$

$$H_\rho \sim \frac{J_1(k\rho)}{k\rho} \sin \psi$$

$$H_\psi \sim \frac{J_1(k\rho)}{k\rho} \cos \psi.$$

On the image plane, $\psi = \pi/2$, the H_z component vanishes. Along the axis, $\rho \to 0$, only the $H\rho$ component remains finite. Therefore, only axial currents occur in the region of the slot. Although the field configuration is more complicated than in a rectangular guide, the action of the slot and probe is similar. The probe couples to the radial field E_ρ, whose dependence is the same as the H_ψ component above, and therefore is a maximum along the vertical probe.

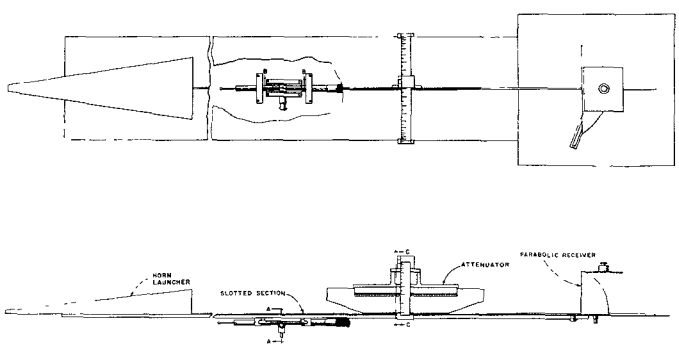

Fig. 9

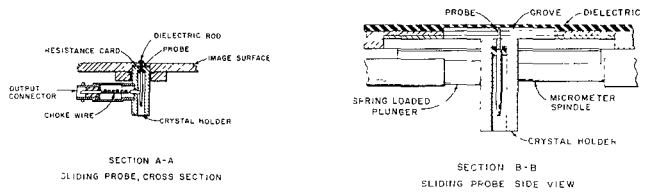

Fig. 10

The design of a slotted standing-wave detector is shown in Figs. 9 and 10. Since the probe extends into a groove in the dielectric, the tolerances on the probe position become critical. This is in marked contrast to the operation of the line as whole, which takes advantage of the extended nature of the wave. In the case of the probe shown, the residual VSWR is about 1 db. There is also evidence of end effects from the slot and the groove in the dielectric.

Directional Couplers

Several types of directional couplers are possible on image line. Perhaps the most obvious is the type proposed by Fox[4] for dielectric waveguides. Here, two guides are curved to bring them gradually in close proximity for a short distance. This method fails for loosely bound waves, because of losses in the necessary bends. By analogy to hollow waveguides, a slot coupling scheme is possible between image lines placed back to back. Here no bends are required; however, multiple slot couplers in the millimeter region demand exacting tolerances.

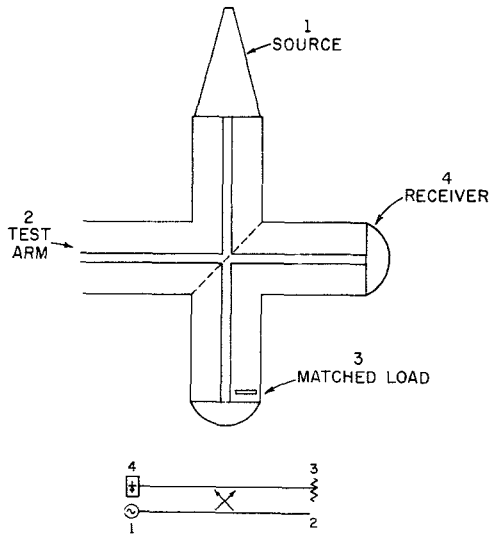

Fig. 11

Neither of the couplers just described makes full use of the properties of the image line. The first uses the wide distribution in the cross section but not the image plane itself; the second takes advantage of the image surface, but couples only in the most critical region of the cross section. An optical directional coupler utilizing a semireflecting surface seems to offer advantages over either of the other types. A sketch of such a coupler is shown in Fig. 11. The actual equipment appears in Fig. 12.

The coupling action takes place over the extended cross section of the wave, and makes good use of the image surface for support and alignment. A sliding short circuit is used to tune out reflections from the reference arm. A small piece of K-band waveguide placed on the image surface serves as the tuning element. Motion of this obstacle along the axis of the dielectric changes only the phase of its reflection; motion perpendicular to the axis changes only the magnitude.

[4] H. G. Fox, "Dielectric waveguide techniques for millimeter waves," Oral paper, IRE Convention, New York, N. Y., 1952.

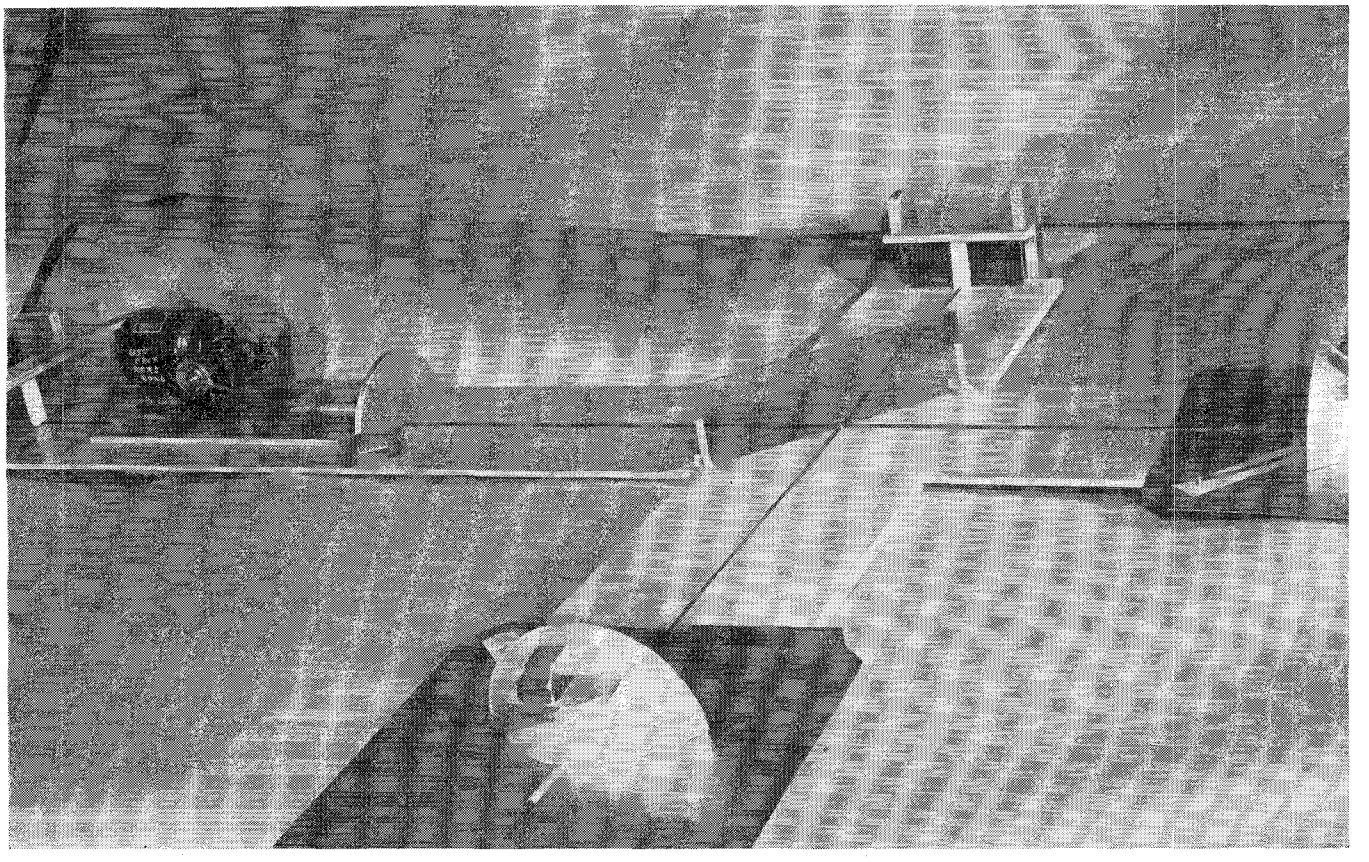

Fig. 12

With this tuning element the coupler could be tuned as a bridge to provide less than $\frac{1}{4}$-db output variation from the sliding short. This corresponds to cross coupling below the 35-db dynamic range available in the present system.

Although tuning is required to achieve this range, this is due to the imperfect reference load used. The coupler itself derives its properties from symmetry, and should not be sensitive to frequency.

Conclusions

A number of circuit elements have been discussed which combine both optical and waveguide principles. At millimeter wavelengths these components offer advantages of low loss and uncritical tolerances. Their relatively large dimensions in terms of wavelengths make them prohibitively bulky at centimeter wavelengths. However, in the millimeter region such large dimensions are generally a blessing.